Smart Mater. Struct. **16** (2007) 2560–2570 doi:10.1088/0964-1726/16/6/060

Transformation fatigue and stress relaxation of shape memory alloy wires

P Pappas[1,2], D Bollas[1,3], J Parthenios[1,3], V Dracopoulos[1] and C Galiotis[1,2,3]

[1] Foundation for Research and Technology Hellas, Institute of Chemical Engineering and High Temperature Chemical Processes, Patras, Greece
[2] Materials Science Department, University of Patras, Greece
[3] Inter-Departmental Programme of Graduate Studies in Polymer Science and Technology, University of Patras, Greece

Received 8 March 2007, in final form 14 August 2007
Published 31 October 2007
Online at stacks.iop.org/SMS/16/2560

Abstract
The present work deals with the stress generation capability of nickel–titanium shape memory alloys (SMAs) under constrained conditions for two well-defined loading modes: recurrent crystalline transformation (transformation fatigue) and a one-step continuous activation (generated stress relaxation). The data acquired will be very useful during the design process of an SMA Ni–Ti element as a functional part of an assembly. Differential scanning calorimetry (DSC) was employed in order to investigate the transformation characteristics of the alloy before and after the tests. Transformation fatigue tests revealed that the parameter that affects more the rate of the functional degradation is the number of crystalline transitions the wire undergoes. Thus, the service life limit of this material as a stress generator can be reduced to a few thousand working cycles. For stress relaxation, the main factor that affects the ability for stress generation is the working temperature: the higher the temperature above the austenite finish (TA_{f}) limit the higher the relaxation effect. Thermomechanical treatment of the alloy during the tests reveals the 'hidden' transformation from the cubic structure (B2) of austenite to the rhombohedral structure of the R-phase. It is believed that the gradual loss of the stress generation capability of the material under constrained conditions must be associated to a gradual slipping relaxation mechanism. Scanning electron microscopy (SEM) observations on *as-received*, re-trained, fatigued and *stress-relaxed* specimens in the martensitic state provide further support for this hypothesis.

(Some figures in this article are in colour only in the electronic version)

1. Introduction

Shape memory alloys (SMAs), under deformed and constrained conditions, exhibit the ability to generate mechanical stress, a characteristic that makes them ideal actuators in several modern applications. SMA-based actuators are capable of replacing complex and heavyweight driving motors with simple and lightweight components. Automotive and aerospace engineering are only two of the fields where SMA-based 'smart' structures can be incorporated in several applications [1]. They can also withstand static or dynamic external loading with their actuating function. The most widely used alloy that exhibits 'shape memory' behavior is the binary nickel–titanium (Ni–Ti) alloy. The wide use of Ni–Ti in the form of rod, strip, tube, spring or wire, as an actuator is mainly due to its ability to generate large mechanical stresses to retrieve large deformations in the range of 6–8% and to be compatible for example with human body tissues. One can also modify its behavior by slightly changing the alloy composition.

The Ni–Ti alloy exists in the form of two different temperature-dependent stable crystalline structures: the high-temperature body centered cubic phase of austenite and the low-temperature monoclinic phase of martensite [2, 3]. If the SMA is deformed while being in the martensitic state, upon

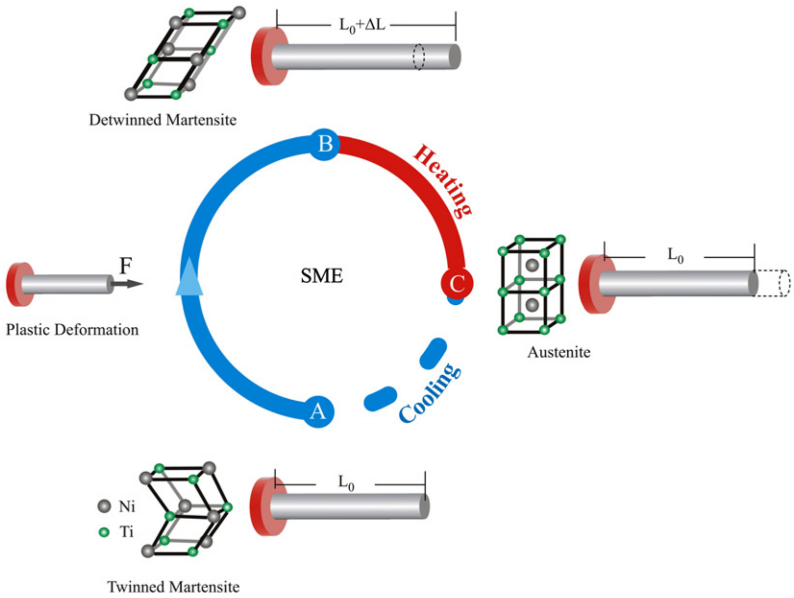

Figure 1. The shape memory effect.

heating, austenite will be formed and the original shape will be restored. During cooling, the inverse crystalline transformation from austenite to martensite will occur, without any change in the shape of the specimen (shape memory effect, SME, figure 1). The maximum recoverable strain reaches 6–8%. Further martensitic deformation results in unrecoverable strain which tends to reduce not only the force generation ability of the SMA material but also its ability to retrieve the original shape. If the SMA material is kept constrained during shape recovery a significant amount of mechanical stress will be induced. In the case of constrained SMA wires, the axial force upon shape recovery can reach values corresponding to 700 MPa of stress [4].

Depending on the way the SMAs are designed to operate in a particular application, their *transformation fatigue* and/or *stress relaxation* under constrained conditions are two important issues that define the operational life of a particular adaptive component. Cyclic loading of an SMA element must be associated with both *structural* and *transformation* (or *functional*) fatigue. Both of them limit the service life of the SMA component [5]. Fatigue of a structural material is the gradual reduction of its ability to support forces under a recurring external mechanical load, leading ultimately to fracture due to accumulating microstructural damage. For example, the accepted fatigue life of an SMA thermal valve is 10^4 cycles and that of an SMA robot gripper is 10^6 cycles [5, 6]. On the other hand, transformation fatigue is a phenomenon that occurs every time the SMA element functions as an actuator. It describes the gradual loss of its ability to generate mechanical stress under constrained conditions and retrieve its shape under cyclic martensitic–austenitic transformation (activation). In this case, the SMA component cannot perform as an actuator although it may be still be effective as a structural element.

Regarding structural fatigue, Tobushi *et al* [7] and Miyazaki *et al* [8] introduced the bending–rotation fatigue test for SMA materials. Duerig *et al* [9] claimed that the bending–rotation test is a good way to predict other types of fatigue behavior. Constant strain amplitude fatigue tests on Ni–Ti wires ($TA_{\mathrm{f}} = 77\,^{\circ}\mathrm{C}$) revealed a fatigue life of 3×10^2 cycles at $125\,^{\circ}\mathrm{C}$ and 3×10^4 cycles at $50\,^{\circ}\mathrm{C}$ for 3% strain amplitude. For 1% strain amplitude, the measured fatigue life was 6×10^3 cycles and greater than 10^6 cycles, respectively [8]. In general, Ni–Ti performs better in fatigue under strain controlled environments but it degrades rapidly under stress controlled experiments. Tobushi *et al* [7] performed bending–rotation tests on Ni–Ti wires and examined the influence of the strain amplitude, the air/water environment and the rotational speed of the assembly. They concluded that the measured relatively long structural fatigue life of Ni–Ti is due to the small size of the material grains. Finally, Tabanli *et al* [10] examined the effect of mean stress during a recurring external load in super-elastic Ni–Ti specimens. Depending on the value of the mean stress, the fatigue life varied from 10^4 to 10^5 cycles.

In the field of transformation fatigue of Ni–Ti shape memory alloys there is no or very little work reported. Eggeler *et al* [5] performed functional fatigue tests on Ni–Ti 0.80 mm diameter springs in order to investigate the fatigue life of Ni–Ti wires under cyclic thermomechanical loading. During the first 100 cycles the actuator spring suffered irreversible plastic deformation in both high and low temperature phases. This effect did not seem to progress further at higher working cycles.

In this paper, we conduct a detailed examination of the transformation fatigue and stress relaxation during activation of Ni–Ti wires under constrained conditions, in terms of the maximum generated axial mechanical stress. The stress relaxation test was conducted at the recommended working temperature of the alloy. The effect of elevated working temperature was recorded by studying the transformation fatigue behavior of the SMA wires at four different thermal environments. Post-experiment differential scanning calorimetry (DSC) tests were employed to assess possible alterations in the transformational characteristics of the tested specimens.

Table 1. Transformation temperatures (measured by DSC).

Heating			Cooling			Hysteresis
TA_s (°C)	TA_f (°C)	TA_p (°C)	TM_s (°C)	TM_f (°C)	TM_p (°C)	$TA_p - TM_p$ (°C)
75	83	79	63	42	52	27

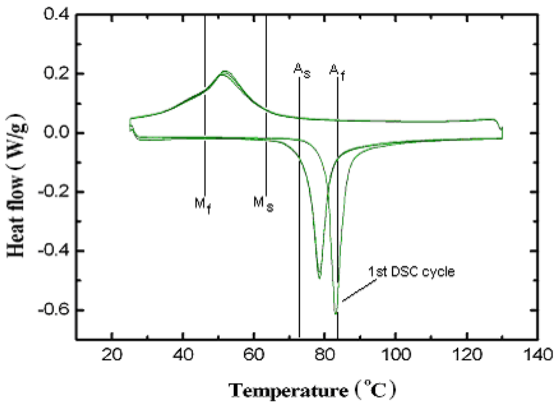

Figure 2. *As-received* Ni–Ti SMA wire DSC test results.

2. Experimental details

The present work was carried out by testing a binary, one-way, shape memory Ni–Ti alloy in the form of a 300 μm diameter cold-rolled wire, with oxidized surface, produced by AMT (Belgium). Based on experimental results derived from tests conducted almost simultaneously with the work presented here [11], the shape memory of the—as-received—wires appears to have been set during the manufacturing process. It is believed that the tested material is well designed to perform as an actuator and, hence, to generate mechanical stress under constrained conditions very close to the maximum level, without prior plastic deformation of the martensite. The transformation characteristics were determined by DSC tests on a TA Instruments apparatus (Q100 model) according to the F2005 ASTM standard [12]. Analysis of the DSC data was performed using the TA Instruments DSC software TA Universal Analysis. During the austenitic transformation upon heating, the *austenite start* (TA_s), the *austenite finish* (TA_f) and the *austenite peak* (TA_p) temperatures of the material were measured. The corresponding temperatures for the inverse transformation into martensite, TM_s, TM_f and TM_p were also determined upon cooling. The pre-test DSC results for the Ni–Ti SMA wire are shown in figure 2. The transformation temperatures, calculated using the tangential method, are also presented in table 1. It is important to note the anomalous shift of the austenitic transformation to higher temperatures which is observed during the first DSC thermal cycle of the SMA specimen.

Before proceeding to the main set of experiments, a few samples of SMA wire were subjected to a re-training procedure [13]. The wires were placed in a fully controlled laboratory oven for 5 min at 510 °C under no external load (0% strain). The re-training procedure aimed at the complete removal of any plastic deformation due to manufacturing or packaging of the product. It is also expected that the re-trained wires will no longer be able to act as force generators unless they are plastically deformed. DSC characterization of these specimens was performed between ambient temperature and 130 °C, following exactly the same cooling and heating rates as those employed in the DSC tests of the as-received material. Finally, the trained wires were activated under constrained conditions in order to confirm the initial premise that the stress generating ability of the as-received wires was due to pre-straining during manufacture.

All transformation fatigue and stress relaxation tests were conducted on a tailor-made experimental system (*THERMIS)* developed for the needs of this project [11]. The system is capable of performing thermomechanical tests on SMAs in the form of wire, strip, rod or tube. It is also capable of testing and characterizing composites incorporating SMAs. As shown in figure 3(a), it consists of several sub-components, capable of real-time data acquisition: (i) a fully controlled and programmable hydraulic mechanical testing system (MTS) to record the mechanical axial stress upon wire activation at fixed strain values, (ii) a thermal IR camera system (Nikon, Thermal Vision Laird 3A) to record the wire surface temperature at specific points and the wire surface temperature distribution, (iii) a fully programmable SMA wire activation device by means of an electric power unit, (iv) a multi-channel temperature recording system using J-type thermocouples obtained from RS, UK and, finally, (v) a specially developed torsional SMA tester mounted on the MTS. It is worth mentioning here that the SMA wire transformation fatigue and stress relaxation experiments do not require real-time recording of the generated mechanical stress, therefore using a mechanical frame such as an MTS was not deemed necessary. Thus, in order to conduct less demanding but time-consuming tests, a portable SMA wire-tester (figure 3(b)) was developed, capable of recording the generated force during activation.

In order to activate the specimen, we take advantage of the wire resistance and the Joule effect, letting a certain amount of electric current pass through the wire and thus raising its temperature. The SMA transformation fatigue tests were carried out using a 120 mm long, 0% pre-strained Ni–Ti wire, kept constrained on the portable device described above. The device was placed into an isolation box to avoid environmental disturbances and to maintain the temperature distribution as uniform as possible. During activation, the maximum temperature of the Ni–Ti wire was just above 110 °C, while the controlled room temperature was maintained at 25 °C by air conditioning. Constrained conditions tend to shift the transformation temperatures upwards [19, 20]. In the case of constrained (embedded in a polymer matrix) Ni–Ti wires it has been found that the TA_f temperature increase does not exceed the range of 5–10 °C, even if the pre-strain level reaches 6% [20]. The difference of about 30 °C between the wire maximum temperature and TA_f is therefore enough to ensure that the austenitic transformation has been completed

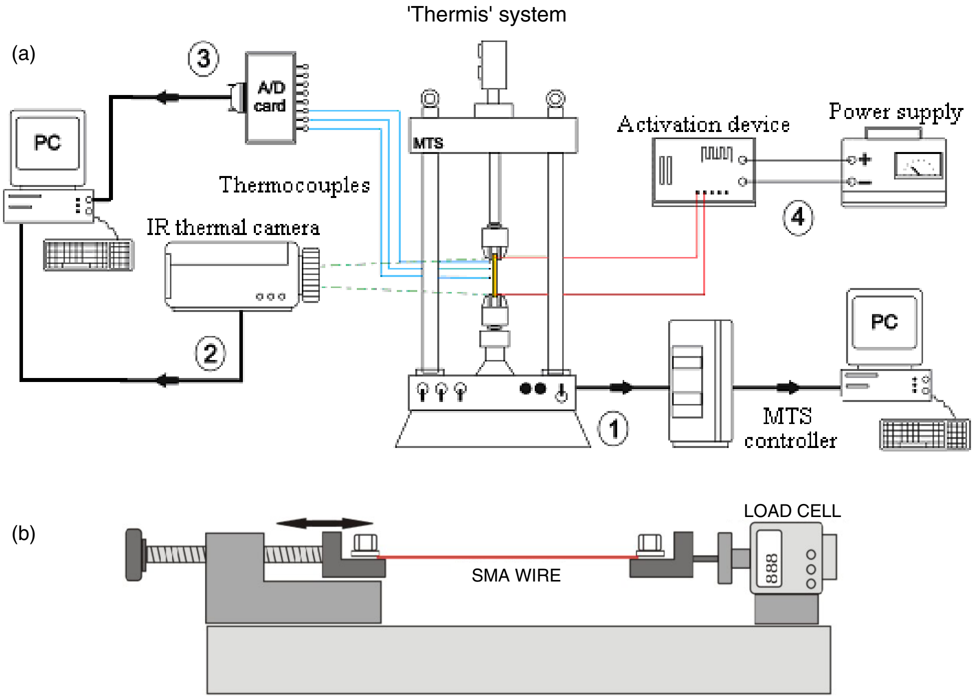

Figure 3. (a) *THERMIS*—thermomechanical characterization system. (b) Portable SMA wire activation force measuring device.

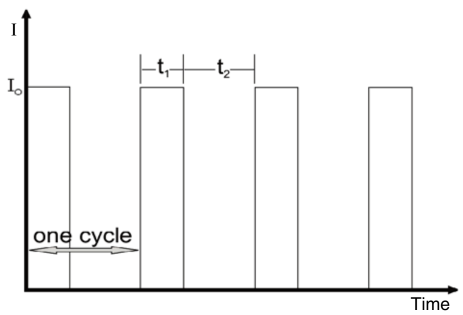

Figure 4. The squared waveform of the activation electric current.

and that the 0% pre-strained SMA wire is fully activated. The applied electric current had the form of a squared waveform (figure 4). The heating time is equal to the pulse duration t_1, while t_2 represents the wire cooling time. Hence, one transformation cycle is completed at $t_1 + t_2$. The cooling time during all experiments was kept constant at 15 s.

Two of the most important parameters affecting the Ni–Ti wire functional fatigue behavior are the number of the transformation cycles the material is subjected to and the activation time (heating time) in each cycle. In order to study how the activation time affects the transformation fatigue behavior of the wires, the experiment was repeated for different *duty cycles, k* [14] as defined below:

$$Duty\ cycle, k = \frac{t_1}{t_1 + t_2}. \tag{1}$$

The mechanical stress relaxation test investigates the ability of the Ni–Ti wires to maintain the generated axial force when activated. After activating the 120 mm long, 0% pre-strained wires, the magnitude of the generated force was being recorded as a function of time. The effect of the working temperature on the stress relaxation was also studied by varying the magnitude of the electric current heating the wires. Similar to the transformation fatigue tests, the SMA wire was kept protected from surrounding air fluctuations and the environment temperature was also kept at 25 °C. In all experiments, the maximum time of continuous activation was 225 h (9.4 days). Prior to testing, unconstrained SMA wires were subjected to a few activation cycles in order to establish a steady functional state.

On completion of the above tests, both types of specimen were subjected to 'post-mortem' DSC measurements, in an attempt to track down possible irreversible changes in the transformational characteristics of the alloy. In addition, aiming to obtain useful information about the thermomechanical fatigue mechanism in the Ni–Ti alloy, four different types of wire specimens were observed using the SEM technique: *as-received* wires, re-trained wires and of course specimens originating from the stress relaxation and fatigue experiments conducted. All the SEM observations were conducted on a Zeiss Supra 35VP system with a field emission gun under a voltage of 10.00 kV.

3. Results

Precise control of the wire temperature was a critical parameter in order to achieve reliable results from both types of test. Relating the wire resistance to temperature is problematic; therefore, the wire surface temperature was monitored by employing sensitive thermocouples and the IR camera. For the 120 mm long Ni–Ti wire, the temperature data were related to

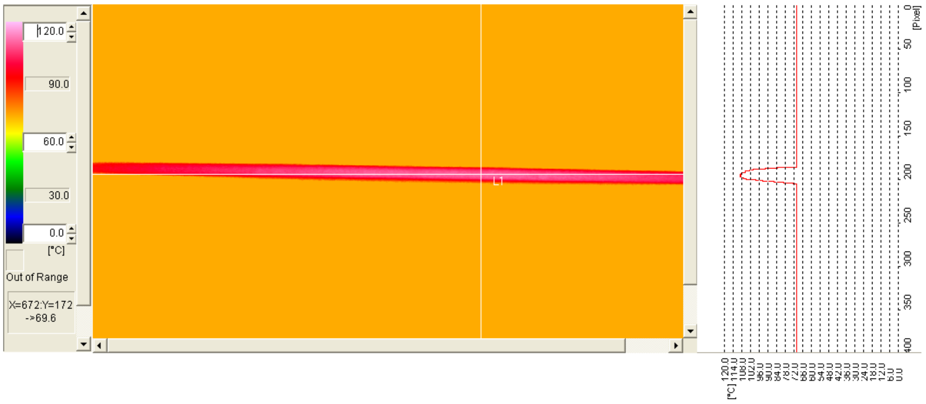

Figure 5. Thermal IR camera image of an activated SMA wire specimen; the temperature distribution from the wire axis to the outside is shown on the right.

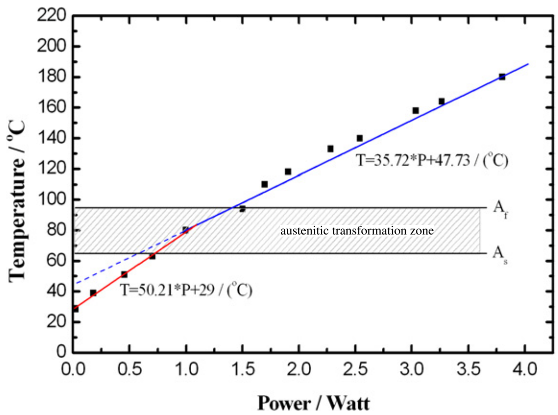

Figure 6. Temperature of a 120 mm long Ni–Ti wire versus electric power.

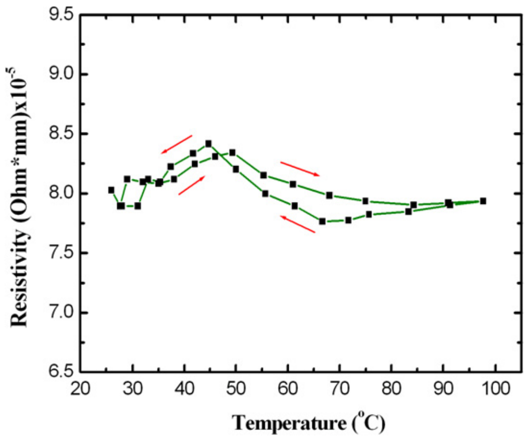

Figure 7. Resistivity of a 0.3 mm diameter Ni–Ti wire versus temperature during heating and cooling.

the amount of electric power required to heat the specimen. In figure 5, the surface temperature distribution of the Ni–Ti test wire is shown. It is clearly visible that the body of the SMA wire is not uniformly heated and that temperature decreases from the inside to the outer surface due to the fact that the specimen is exposed to the open air. It is expected that the temperature at the center of the wire is a few degrees higher than that measured by using thermocouples on the surface.

In figure 6, the recorded temperature of the wire surface at the middle of its length is plotted as a function of the input power; the results can be considered as exhibiting two linear relationships corresponding to martensite and austenite phases, respectively. If this relationship holds true, then, inversely, the resistance of the two phases can be estimated by conducting independent temperature measurements. Since the working temperature for all fatigue and stress relaxation tests was well above TA_f, it is reasonable to employ a linear equation, which for the austenite region is given by

$$T = 35.72 \cdot P + 47.73, \qquad T > TA_f, \tag{2}$$

where T stands for temperature in °C and P stands for electric power in watts. Equation (2) is only valid for a 120 mm long wire. The electric power is proportional to the resistance of the wire. The resistance is also proportional to the length of the wire, according to

$$R = \rho * \frac{L}{A} \tag{3}$$

where ρ stands for resistivity, A is the cross-sectional area of the wire, and L stands for wire length. By testing unconstrained *as-received* Ni–Ti wires on the *THERMIS* system it was made possible to measure the alterations of the resistivity, ρ, during activation, as well as the hysteresis effect upon cooling. The results are presented in figure 7. From the above, it follows that the temperature is proportional to the electric power and that the electric power is proportional to the wire length. This makes it possible to predict and control the temperature of a 0.3 mm diameter Ni–Ti wire in the open air by adjusting the input electric power (equation (2)).

3.1. Re-trained wire tests

The DSC results for the trained SMA wires are presented in figure 8. It is obvious that the shift observed earlier (figure 2) of the austenitic transformation to higher values at the first thermal cycle is also obtained here. On cooling, as the martensitic transformation takes place, two different crystalline transitions are present, as manifested by the two peaks in the

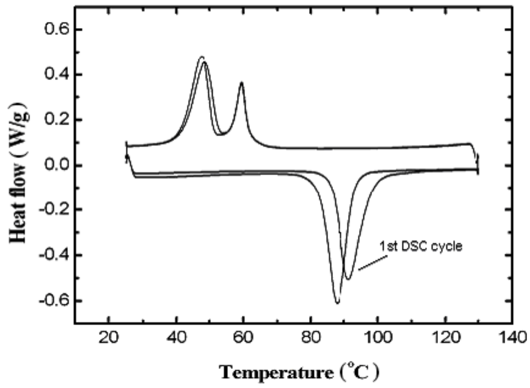

Figure 8. DSC graph of trained wires.

DSC graph. Also, there is an increase of the 'transformation window' to higher temperatures.

The DSC tests were followed by thermal activation experiments aiming to investigate the force acting ability of the undeformed trained wires. Using the *THERMIS* system, it was reasonable to confirm that the wires were not capable of generating mechanical stress at 0% elongation due to the shape memory effect. For higher strain levels (3% and 6%) under constrained conditions a significant amount of stress was produced during shape memory recovery.

3.2. Stress relaxation experiments

As shown in figure 9(a), the generated axial mechanical stress decreases with activation time (continuous operation) in all four cases tested here. After 225 h of activation for each SMA specimen at 116 °C, 138 °C, 156 °C and 164 °C, the wire was capable of generating 85%, 70%, 50% and 45% of its initial stress, respectively. The reduction rate of the generated mechanical stress strongly depends on the activation temperature. This effect is best viewed in figure 9(b), in which the rate of generated axial mechanical stress as a function of heating time is presented. During the first 24 h of activation at maximum stress level, the Ni–Ti wire has lost 12% (at 116 °C), 20% (at 138 °C), 32% (at 156 °C) and 39% (at 164 °C) of its maximum force acting capability. The experimental results were fitted using an appropriate two-parameter equation. Since stress values are normalized the maximum generated axial stress at the beginning of the test is set to 1. Corresponding fitting curves are also presented in figure 9(a).

3.3. Transformation fatigue experiments

The transformation fatigue experiments were performed for different *duty cycles*, k, of 0.44, 0.50, 0.53 and 0.57. All four tests were conducted at 1.904 W, corresponding to an estimated temperature of 116 °C. The maximum generated axial stress was 520–535 MPa for the first activation cycle. The gradual reduction of maximum axial stress as a function of transformation cycles is shown in figure 10. The vertical axis values are normalized to the maximum observed stress of each wire in order to eliminate possible fluctuations in the values of maximum generated stress between specimens.

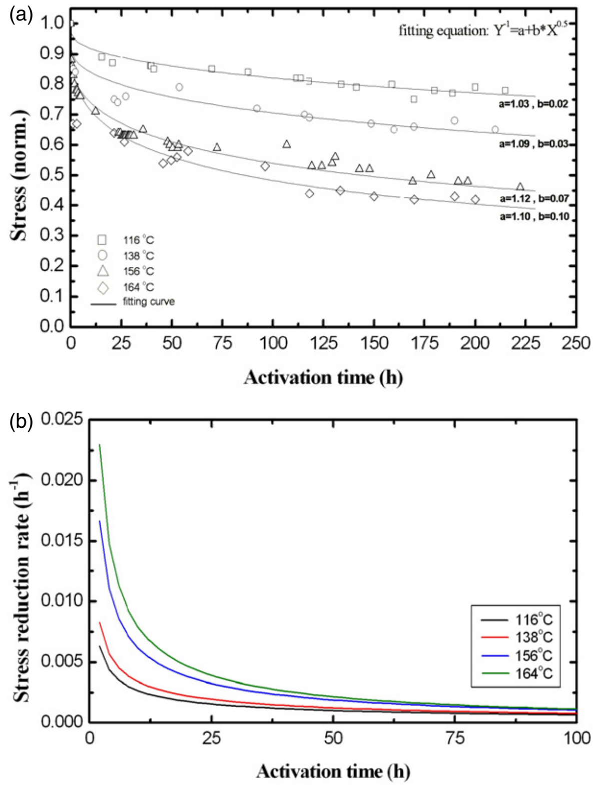

Figure 9. (a) Generated stress relaxation experimental results and fitting curves. (b) Stress relaxation experiment: maximum generated stress rate.

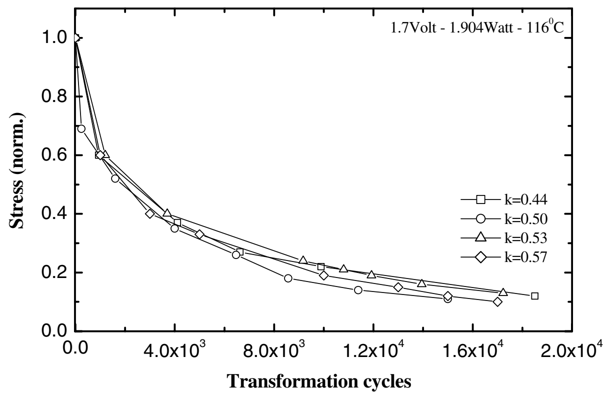

Figure 10. Transformation fatigue experiment: maximum generated stress.

By fixing the cooling time t_2, it is evident that the *duty cycle* is only affected by the heating time t_1, which can be considered as the actuator 'activation' time. As shown in figure 10, the experimental stress data decrease with the number of transformation cycles regardless of the different values of *duty cycle*, k. Re-testing the specimens after a few days indicated that the SMA wires exhibited a complete loss of the ability to exercise force upon activation.

The transformation fatigue experimental data were fitted using a two-parameter exponential function. Each set of data was processed separately and an average fitting equation was derived. The fitting curve vis-à-vis the experimental data are

Table 2. DSC results.

	DSC values										
	Austenitic transformation					Martensitic transformation					
Specimen	A_s (°C)	A_p (°C)	A_f (°C)	Latent heat (J g^{-1})	$A_f - A_s$ (°C)	M_s (°C)	M_p (°C)	M_f (°C)	Latent heat (J g^{-1})	$M_f - M_s$ (°C)	Hyster. (°C)
As-received	73.33	78.68	82.66	17.37	9.33	62.53	51.82	43.63	15.08	18.9	26.86
Fatigue $k = 0.44$	77.58	81.02	84.93	20.70	7.35	59.91	55.58	48.04	19.49	11.87	25.44
Fatigue $k = 0.53$	77.50	81.18	84.43	21.26	6.93	60.42	55.52	47.61	19.64	12.81	25.66
Relaxation 138°C	79.07	87.83	91.83	26.24	12.76	69.94	52.80	39.60	25.55	30.34	35.03
Relaxation 156°C	79.75	87.91	93.86	27.34	14.11	66.32	60.13	38.99	26.62	27.33	27.78
Relaxation 164°C	80.42	89.25	94.99	15.10	14.57	65.13	58.86	37.94	19.38	27.19	30.39

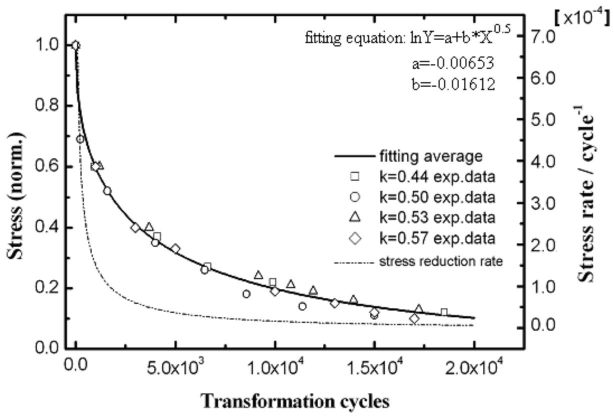

Figure 11. Transformation fatigue fitting curve and stress reduction rate during the experiment.

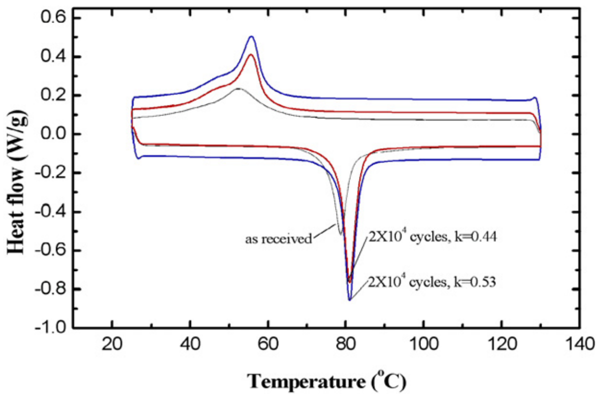

Figure 12. Transformation fatigue—post-test DSC graphs.

shown in figure 11. After 20.000 transformation cycles the SMA wire can no longer perform as an actuator since it is not capable of producing an efficient amount of axial mechanical stress under constrained conditions. The half-life of the fully activated wire appears at about 2.000 transformation cycles. At 4.000 transformation cycles the SMA wire reaches the limit of its service life. The reduction rate of maximum generated mechanical stress as a function of transformation cycles is also presented in figure 11. The maximum stress rate is related to the intensity of the transformation fatigue mechanism. As is apparent, the stress generation ability of a constrained SMA wire under cyclic thermomechanical loading exhibits an abrupt decrease in the first few hundred transformation cycles.

3.4. Post-test DSC measurements

The DSC curves of an untested Ni–Ti wire and of two SMA wires subjected to 2×10^4 transformation cycles for $k = 0.44$ and $k = 0.53$ are shown in figure 12. It is worth noting here that after the fatigue experiment the tested wires were not capable of generating a maximum stress of over 30–40 MPa (2–3 N axial force). The results of the DSC experiments are presented in table 2. During heating, there was a shift of the austenitic ‘transformation window’ to higher temperatures followed by an increase in the latent heat of the crystalline transformation. The same effect was observed during the reverse martensite transformation on cooling of the specimens. Finally, it is interesting to note that both austenitic (TA_f–TA_s) and martensitic (TA_f–TA_s) transformation temperature ranges were shortened.

Regarding generated stress relaxation, the DSC curves of an untested Ni–Ti wire and of three SMA wires stress-relaxed for 225 h at 138 °C, 156 °C and 164 °C, respectively, are shown in figure 13, and the results are also presented in table 2. The austenitic ‘transformation window’ exhibited a large shift of about 10 °C, which tends to increase in respect to the working temperature. The latent heat of both transformations also increased, while there was a large broadening of the transformation temperature range. Unlike the case of the fatigue experiments examined earlier, the obtained Hysterisis became more pronounced. On cooling, two different peaks were revealed, corresponding to two different crystalline transformations which may be linked to the presence of the R-phase structure [15].

4. Discussion

As is apparent from the transformation fatigue data, for a fixed cooling time t_2, the maximum generated mechanical stress of the SMA wires is insensitive to the duty cycle parameter, k.

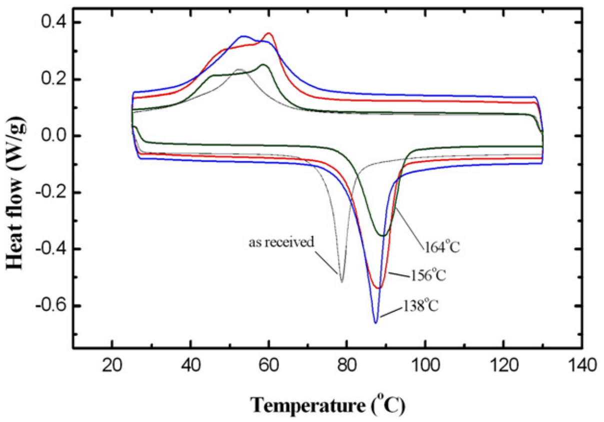

Figure 13. Stress relaxation—post-mortem DSC graphs.

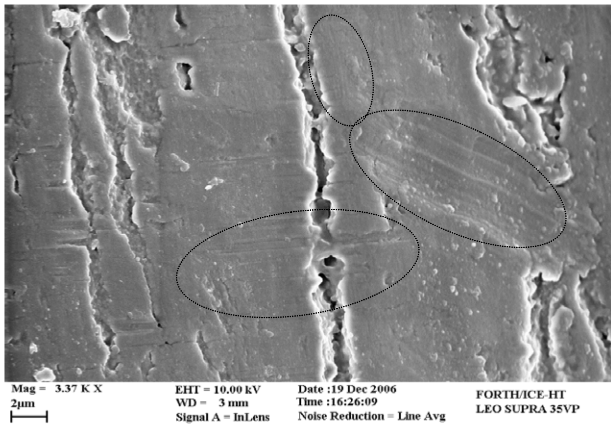

Figure 15. SEM image obtained from a re-trained Ni–Ti wire.

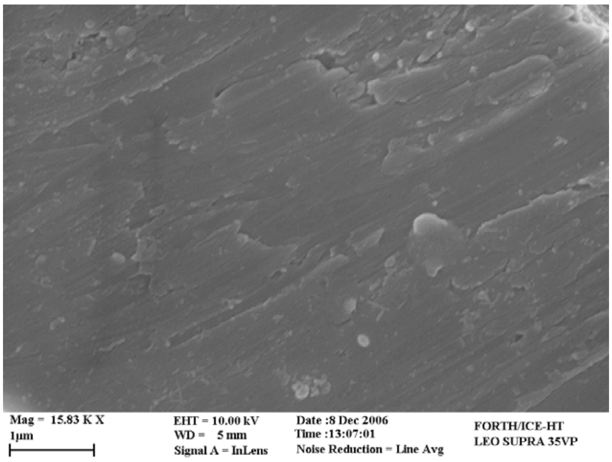

Figure 14. SEM image obtained from an *as-received* Ni–Ti wire.

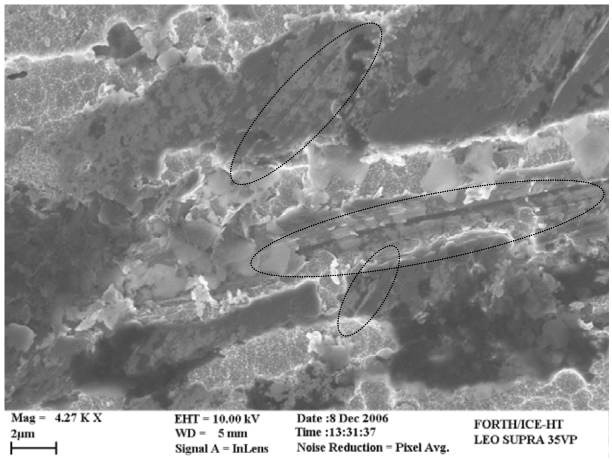

Figure 16. SEM image obtained from a specimen subjected to thermomechanical fatigue.

It thus follows that the magnitude of the 'activation' time, t_1, is not a critical parameter during transformation fatigue of the SMA wire. In contrast, the decreasing function of stress with transformation cycles indicates that the frequency of the martensite–austenite–martensite transformation is the most critical damaging parameter for this material. The maximum stress reduction rate is observed during the initial phase of the transformation fatigue tests and remains almost constant after the half-life of the wire at 2000 cycles. The SMA wires were able to generate only a small amount of pulling force of about 1–2 N after the tests. However, when activated, they were capable of a complete shape recovery under no external load. This is evident in the post-mortem DSC curves, where the crystalline transformation from martensite to austenite and vice versa is very clear regardless of the observed changes in the wire characteristics. Hence, the loss of the force acting ability should not be due to the loss of the shape memory effect for an SMA material. The Ni–Ti material responds to an applied stress by changing the orientation of its crystal structure through movement in the regions of the twin boundaries. When the deformed material is activated, it is the same mechanism above that induces geometry changes and under constrained conditions produces mechanical stress.

In order to throw light on the mechanism that is responsible for the loss of stress generation in fatigued specimens, we have examined by means of high resolution SEM the as-received material (which has been found to possess a certain amount of pre-strain), a re-trained wire and two specimens after the transformation fatigue and stress relaxation experiments. The results are presented in figures 14–17 respectively, and as can be seen the uniform grain orientation characterized by previous authors as POM (preferentially oriented martensite) [16] is definitely present in the pristine material but the re-trained wire and both of the tested specimens have structural features that resemble self-accommodated martensite (SAM). However, the DSC experiments revealed distinct differences between a pure SAM specimen and that received after the fatigue or the stress relaxation experiment. In other words, during transformation fatigue or stress relaxation, the oriented martensite variants relax at high temperatures and under constrained conditions and, as a result, they revert back to specimens that incorporate a SAM-like structure. On the other hand, pure self-accommodated martensite variants can be observed in the structure of the re-trained material as a result of the intense thermal treatment. We postulate that under constrained transformation fatigue a slip mechanism that affects mostly the twin boundary regions operates and the material in effect loses the initial pre-strain. Indeed the DSC measurements

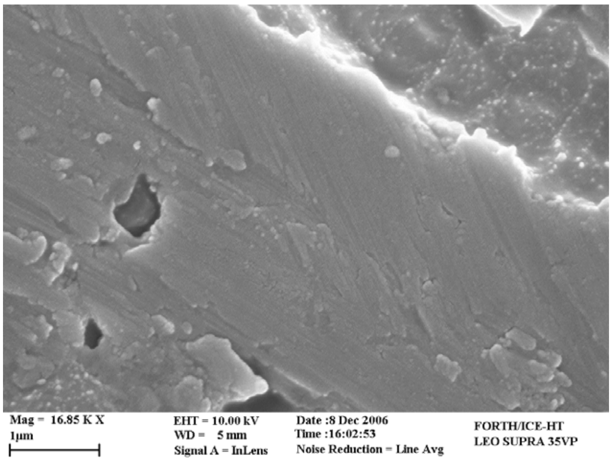

Figure 17. SEM image obtained from a *stress relaxed* Ni–Ti wire.

mentioned above confirm that no other degradation mechanism has taken place. Constrained thermomechanical cycling undoubtedly induces defects and dislocations; however, full crystallographic reversibility from martensite to austenite is difficult to be achieved even in stress-free transformations [17]. In figure 18, the scheme of the proposed mechanism is presented for both types of experiment performed here.

During stress relaxation experiments under constrained conditions, the specimen is constantly under tensile load and, therefore, the generated axial force decay with respect to time is most likely affected by slipping movements in the regions of the crystal boundaries within the oriented phase of the material. This again indicates that the loss of the initial pre-strain is also the reason for the loss of stress generation in this case. There is no doubt that, during continuous activation of a Ni–Ti SMA wire, the most important parameter is the working temperature. All four stress relaxation experiments were conducted at temperatures well above the austenitic transformation zone and it was found that, for test conditions close to TA_f, the generated stress degradation is much less intense compared to that taking place at higher working temperatures. Consequently, the highest stress reduction rates are observed at the highest working temperatures, and like the case of transformation fatigue, the stress relaxation rate reaches its maximum during the initial phase of the test. Although the nature of the stress relaxation and the transformation fatigue experiments is different, it would be of great interest an attempt to 'link' the experimental results. Taking into account that in both cases the SMA wire is fully activated and thus it generates its maximum axial force, then, the transformation cycles can be 'converted' into continuous activation time as follows:

$$\text{continuous activation time} = i \times t_1$$

where i stands for the number of the transformation cycles and t_1 stands for the cycle activation time which differs for

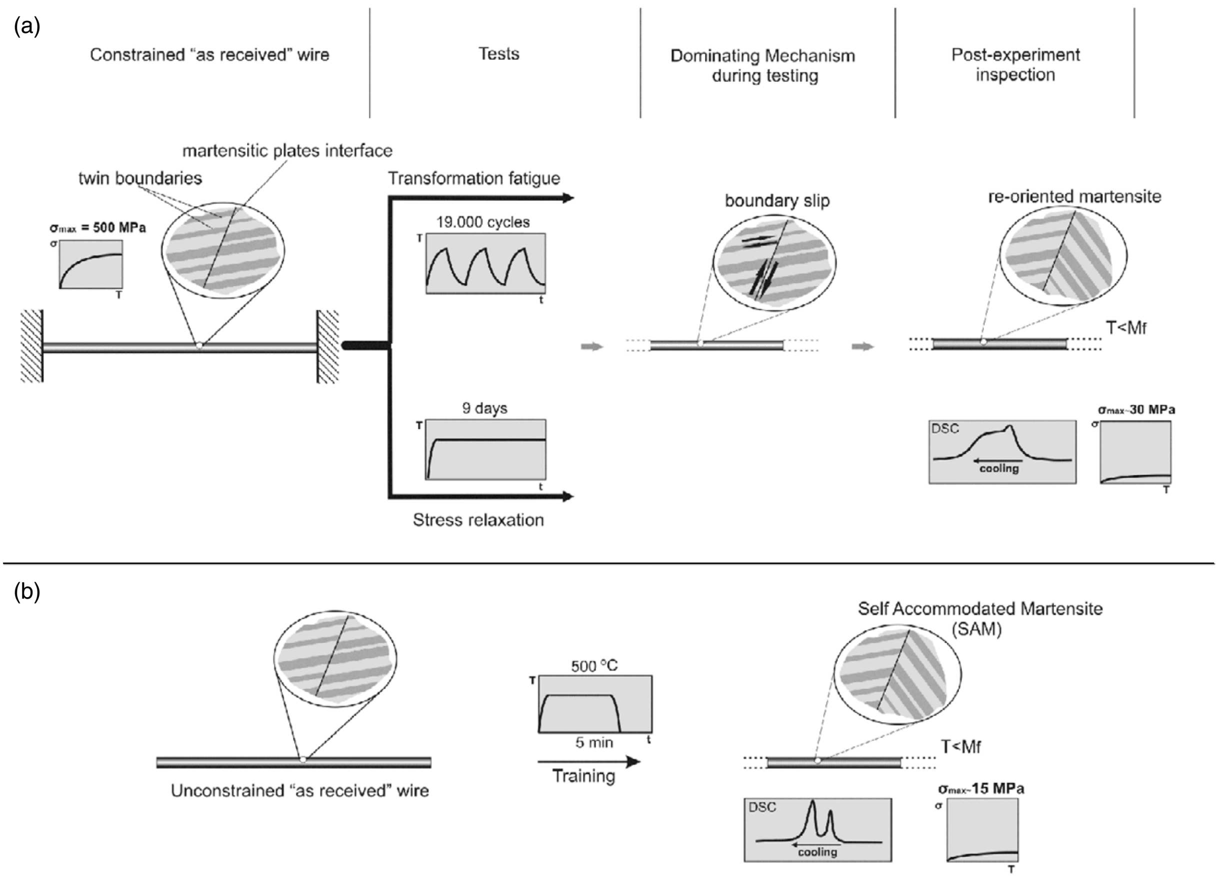

Figure 18. (a) Proposed mechanism during transformation fatigue and stress relaxation and (b) SAM formation after re-training of the wire.

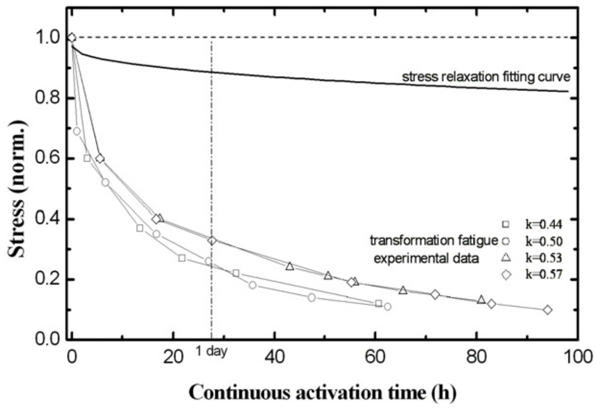

Figure 19. Transformation fatigue and stress relaxation in terms of continuous activation time.

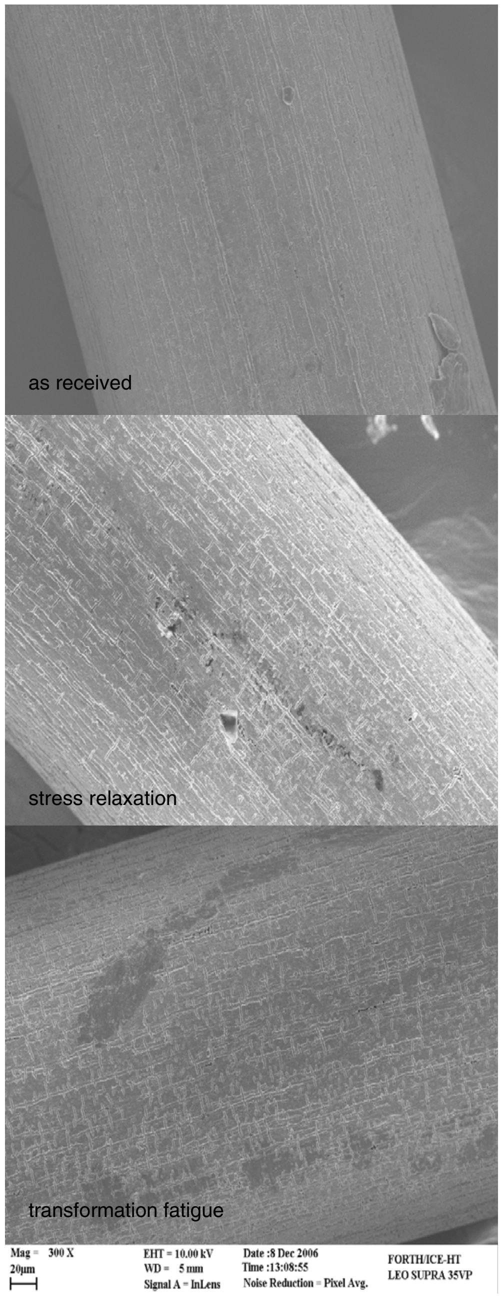

Figure 20. Ni–Ti wire surface SEM image for three different specimens: *as-received* wire, *stress-relaxed* wire and *transformation-fatigued* wire.

each duty cycle, k. Transformation fatigue experimental data and stress relaxation fitting curve (at 116 °C) versus continuous activation time are presented in figure 19. Since the generated maximum stress rate is much slower than that obtained from the fatigue data, it can assumed that the cyclic transformation process is more detrimental, as far as the decay of generated stress is concerned, than that obtained from the stress relaxation experiment.

Post-mortem DSC measurements revealed a certain alteration of the wire transformational characteristics. The fatigued specimens exhibited a shortened martensitic and austenitic transformation temperature range, in association with only slight changes in Hysterisis. As a result, although the Ni–Ti wires were unable to generate stress, there was a much quicker crystalline transition both ways. For the stress-relaxed specimens, during cooling when martensite is formed, two different peaks are observed. Taking into account the fact that the tested SMA wires were thermomechanically treated for a long time at elevated temperatures [15], it is believed that the first peak, which was present to higher temperatures, is related to the crystalline transformation from the cubic structure (B2) of austenite to the rhombohedral structure of the R-phase. Although there have been many studies in the past [21] it is true that the real crystal structure of this intermediate phase is still controversial. The second peak corresponds to the transformation from the R-phase to the monoclinic structure (B19′) of martensite. Unlike the fully annealed and quenched Ni–Ti materials (such as the tested *as-received* wires) which transform directly from the B2 phase to the B19′ phase, thermomechanically aged alloys transform in two stages (B2 $\rightarrow$ R $\rightarrow$ B19′). In later studies this behavior is attributed to the inhomogeneous precipitate distribution between the grain boundary and the grain interior [18].

The trained wire DSC experiments provided useful information about the material tested in this project. Due to the high temperature (510 °C) heat treatment of training, the R-phase transition is clearly visible via the two distinct and intense peaks during the cooling stage. The presence of the austenitic transformation temperature shift is strong evidence towards dissociating this phenomenon from plastic martensitic deformation which is removed when the specimen is heated for the first time because, prior to testing, all samples were heated above TA_{f} in unloaded conditions. Moreover, the thermal treatment of training results in a completely new material whose attributes are not any longer governed by the manufacturing technique or other fabrication characteristics. The austenite forming temperature shift in the first cycle may be well associated with increased energy absorption in order for the crystalline transition to initiate. The fact that the trained samples, when not deformed, are not capable of producing axial force, unlike the wires used in the transformation fatigue and stress relaxation experiments, indicates that the material purchased was already programmed to retrieve its shape and produce maximum stress.

Finally, in figure 20 an image of the surface of the untested SMA wire magnified is compared to that of specimens that have undergone the tests described in this work. As is evident, both specimens that have undergone transformation fatigue and stress relaxation at high temperatures suffer from extensive surface microcracking as compared to the pristine specimens. Furthermore, as expected, the microcrack density is higher for the wire that has been subjected to transformation fatigue. However, subsequent tensile tests on all these specimens have proved that the tensile mechanical properties are not affected by the increase in surface crack density and therefore this cannot be the primary degradation mechanism for the experiments described here. A crack initiation and propagation mechanism has been found before and discussed by other authors [17].

5. Conclusions

The aim of the present work was to examine some of the functional characteristics of the Ni–Ti shape memory alloy, in order to investigate its ability to work as an actuator in several applications. The degradation of the stress generation ability of the material after recurrent activations (transformation fatigue) and the decrease of the generated actuating force during continuous heating (stress relaxation) are two important matters that should be considered.

Transformation fatigue and stress relaxation experiments were conducted on Ni–Ti SMA wires. The transformation fatigue test consisted of 2×10^4 cyclic crystalline transformations at maximum generated stress for different duty cycles, k. The maximum generated stress fatigue behavior was not affected by the value of k, but only by the frequency of the crystalline transitions between martensite and austenite. The generated stress curve followed the form of an exponential decay.

The maximum generated mechanical stress relaxation is a phenomenon that seems to depend strongly on the working temperature. The relaxation rate is more intense for higher temperatures while the most damaging period for the specimen is the first few hours of continuous activation. Post-test DSC experiments for both cases reveal significant alterations to the transition characteristics of the SMA material but do not indicate a loss of the shape memory recovery ability. Thermomechanically aged wires provide strong evidence related to the presence of the R-phase transformation.

After a long period of activation (either cyclic or continuous) under constrained conditions the Ni–Ti material loses its ability to act as a force generator although the martensitic transformation still occurs during heating. SEM observations confirmed that the main mechanism responsible for the loss of the stress generation ability is the vanishing of preferentially oriented martensite within the wire structure, due to the gradual slipping of martensite variants over the twin boundary regions. In effect the material reverts back to unoriented self-accommodated martensite under fixed constrained conditions at temperatures higher than TA_f.

References

[1] Boller C 1999 *Ann. Mtg of the Materials Research Society (Boston, Dec. 1999)*

[2] Duerig T W, Melton K N, Stöckel D and Wayman C M 1990 *Engineering Aspects of Shape Memory Alloys* 1st edn (London: Butterworth–Heinemann)

[3] Paula A S, Canejo J P H G, Martins R M S and Braz Fernandes F M 2004 *Mater. Sci. Eng.* A **378** 92–6

[4] Stalmans R, Tsoi K and Schrooten J 2000 *5th European Conf. on Smart Structures and Materials*; *Proc. SPIE* **4073** 88–96

[5] Eggeler G, Hornbogen E, Yawny A, Heckmann A and Wagner M 2004 *Mater. Sci. Eng.* A **378** 24–33

[6] Hornbogen E 2004 *J. Mater. Sci.* **39** 385–99

[7] Tobushi H, Hachisuka T, Yamada S and Lin P H 1997 *Mech. Mater.* **26** 35–42

[8] Miyazaki S, Mizukoshi K, Ueki T, Sakuma T and Liu Y 1999 *Mater. Sci. Eng.* A **273–275** 658–63

[9] Duerig T, Pelton A and Stockel D 1999 *Mater. Sci. Eng.* A **273–275** 149–60

[10] Tabanli R M, Simha N K and Berg B T 1999 *Mater. Sci. Eng.* A **273–275** 644–8

[11] Pappas P *et al* 2007 Thermomechanical characterization system for shape memory alloys and hybrid composites *Smart Mater. Struct.* submitted

[12] ASTM 2005 Standard terminology for nickel–titanium shape memory alloys *ASTM Standard* F2005

[13] www.sma-inc.com, information sheet #6, setting shapes in NiTi

[14] Waram T C 1993 *Actuator Design Using Shape Memory Alloys* 2nd edn (Canada: Mondotronics, Inc.)

[15] Tan L and Crone W C 2004 *Scr. Mater.* **50** 819–23

[16] Zheng Y, Schrooten J, Cui L and Humbeeck J V 2003 *Acta Mater.* **51** 5467–75

[17] Lopez H F 2001 *Mater. Lett.* **51** 144–50

[18] Chrobak D and Stroz D 2005 *Scr. Mater.* **52** 757–60

[19] Zheng Y J, Schrooten J, Tsoi K A and Stalmans R 2002 *Mater. Sci. Eng.* A **335** 157–63

[20] Tsoi K A, Stalmans R and Schrooten J 2002 *Acta Mater.* **50** 3535–44

[21] Khalil-Allafi J, Schmahl W W and Toebbens D M 2006 *Acta Mater.* **54** 3171–5